International Journal of Mass Spectrometry 195/196 (2000) 225–237

Dehydration of ionized propanol in the gas phase

Guy Bouchoux[a,]*, Nadège Choret[a], Robert Flammang[b]

[a]*Département de Chimie, Laboratoire des Mécanismes Réactionnels, UMR CNRS 7651, Ecole Polytechnique,*
91128 Palaiseau cedex, France
[b]*Laboratoire de Chimie Organique, Université de Mons-Hainaut, 20 Place du Parc, 7000 Mons, Belgium*

Received 7 June 1999; accepted 18 August 1999

Abstract

Experimental and theoretical reexamination of the dehydration reaction of ionized propanol, **1**, indicates that both ionized cyclopropane and ionized propene are produced as fragment ions. Tandem mass spectrometry experiments including charge stripping, neutralization–reionization, and ion–molecule reactions with ammonia and NO are best interpreted by the formation of a mixture of $[C_3H_6]^{\cdot+}$ fragment ions. The composition of this mixture is nearly insensitive to the internal energy of the precursor ions **1**. Molecular orbital calculations, conducted at the G2(MP2,SVP) level, confirm that the first step of the reaction is the 1,4-hydrogen migration $[CH_3CH_2CH_2OH]^{\cdot+}$, **1** → $[CH_2CH_2CH_2OH_2]^{\cdot+}$, **2**; excellent agreement is found with the experimental critical energy barrier for this reaction. The distonic ion **2** may lead to ionized cyclopropane via a slightly stabilized ion-neutral complex, **3**; the energy determining step of the cyclopropane formation is the dissociation of complex **3**. The second dissociation process of **2**, leading to ionized propene, is associated with a 1,2-hydrogen migration leading to the distonic ion $[CH_3CH(OH_2)CH_2]^{\cdot+}$, **4**; the isomerization **1** → **4** is the energy determining step of this reaction. Starting from **2**, formation of ionized cyclopropane needs 69 kJ/mol whereas the critical energy for ionized propene formation is only 54 kJ/mol. From a strictly energetic point of view, both reactions are allowed for ions **2** coming from **1**, moreover propene ion formation should be favoured. Statistical rate constant calculations using an orbiting transition state model for the dissociation of the loose structure **3**, demonstrate that the two reaction channels in competition at low, as well as at high, internal energy of the precursor ions **1**. (Int J Mass Spectrom 195/196 (2000) 225–237) © 2000 Elsevier Science B.V.

Keywords: Propanol$^{\cdot+}$; Dehydration mechanism; $[C_3H_6]^{\cdot+}$; G2(MP2,SVP) calculations; Collisional mass spectrometry; Ion–molecule reactions

---

1. Introduction

Elimination of water is one of the most important reactions of ionized alcohols. The behaviour of ionized propan-1-ol, **1**, is representative of this class of reactions and, for this reason, it has been the subject of several mass spectrometric and theoretical studies [1–9] (Scheme 1).

Deuerium labeling experiments demonstrate that the loss of water proceeds by a specific and irreversible migration of one hydrogen from the methyl group to the oxygen atom [1,2]. This 1,4-H migration affords the distonic ion $[CH_2CH_2CH_2OH_2]^{\cdot+}$, **2** which may be also produced, for example, by dissociative ionization of 1,4-butane diol and studied separately. It has been shown that both metastable ions **1** and **2**

---

* Corresponding author. E-mail: bouchoux@dcmr.polytechnique.fr

Dedicated to the memory of Professor Robert R. Squires.

PII S1387-3806(99)00177-3

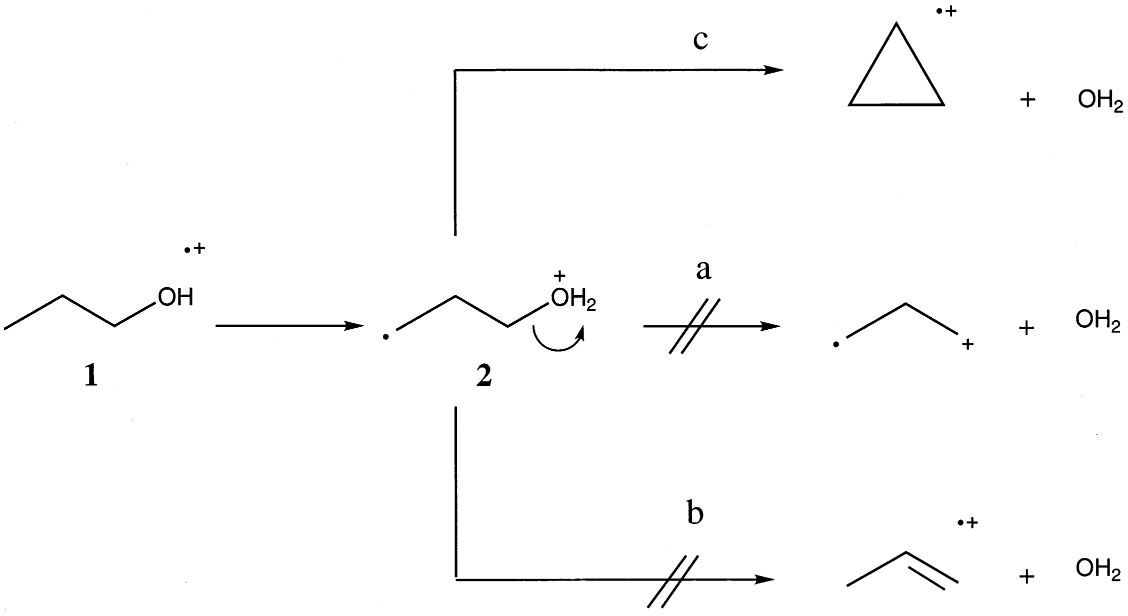

Scheme 1.

eliminate a water molecule [1]. However, structures **1** and **2** are distinct species that may be characterized by their collisional [1–3] or neutralisation–reionization [4] mass spectra. All these results are understandable if the 1,4-hydrogen atom migration **1** → **2** occurs through a transition structure that is the highest point in the path connecting **1** to its dehydration products. Determination of the appearance energy for the $[C_3H_6]^{\cdot+}$ fragment ions, produced by photodissociation of propanol, has been carried out [5] thus providing an accurate value for the energy barrier **1** → **2**.

There are conceptually three means for **2** to expel a water molecule (Scheme 1). Direct elimination of H_2O leading to a distonic $[CH_2CH_2CH_2]^{\cdot+}$ ion (Scheme 1, path a) is not expected because this species is not a stable structure but, rather, a transition state connecting ionized propene and ionized cyclopropane [10]. In order to avoid the formation of a primary carbocation, the neutral loss may be assisted by either a 1,2-H shift (Scheme 1, path b), or a cyclisation process (Scheme 1, path c). In fact, the cyclopropane structure has been assigned to the $[C_3H_6]^{\cdot+}$ fragment ions coming from dissociation of **1** on the basis of its charge stripping mass spectrum [1,2]. This seems surprising because ionized propene is more stable than ionized cyclopropane by 45 kJ/mol. It may also reveal important energetic or kinetic effects during the competition between paths b and c.

Two theoretical studies have been previously devoted to the fragmentation of ionized propanol [8,9]. None of them have explored the possibility of formation of ionized propene. The goal of the present work is to provide new insights into the reaction mechanism and energetics of the water loss from ionized propanol, **1**, by means of (1) new tandem mass spectrometry experiments on ionized propene and cyclopropane, (2) ab initio molecular orbital calculation at the G2(MP2,SVP) level, and (3) statistical rate constant calculations of the various possible reaction routes.

2. Experiments and computations

All the mass spectra were recorded on a large scale tandem mass spectrometer (Micromass AutoSpec 6F, Manchester) combining six sectors of $E_1B_1c_1E_2c_2c_3E_3B_2c_4E_4$ geometry (E, electric sector; B, magnetic sector; c, collision cell) [11]. General conditions were: 8 kV accelerating voltage (unless otherwise stated), 200 mA trap current, 70 eV ionizing electron energy, and 200 °C ion source temperature. Propanol was introduced into the ion source via a heated (180 °C) septum inlet, whereas propene and cyclopropane were introduced via the gas line used in chemical ionization mode.

Collisional activation (CA) and charge stripping (CS) spectra were recorded by scanning the field of E_3 after collisional activation with oxygen in the collision cell c_3. Neutralisation reionization (NR) mass spectra were obtained by neutralizing the beam of selected ions with xenon in c_2 and performing reionization fragmentation with oxygen in c_3, with unneutralized ions being removed by floating an intermediate calibration source at 9 kV. In all these experiments, the product ions were collected in the fifth field-free region with an off-axis photomultiplier detector. In the MS/MS/MS experiments, ions produced in the field-free region situated between B_1 and E_2 were selected by reducing the field of E_2 and scanning E_3.

The installation of an rf-only quadrupole collision cell inside the instrument, between E_2 and E_3, has also been reported elsewhere [12]. In this configuration, the neutralization cell c_2 is replaced by a demagnification lens. The experiments using the quadrupole consist of the selection of a beam of fast ions (8 kV) with the first three sectors, the retardation of these ions to ≈5 eV, and the reaction with a reagent gas in the cell. The pressure of the reagent gas in the cell is estimated to be around 10^{-3} Torr. After reacceleration to 8 kV, all the ions present in the quadrupole are recorded by scanning the field B_2. High energy CA spectra of mass selected ions can also be recorded by a linked scanning of the fields of the last three sectors (EBE, resolved mode) or by a conventional scanning of the field of the last electric sector after mass selection with the second magnet.

The comparison of the various collisional decomposition spectra was done using a similarity index [13], SI, calculated by the relationship:

$$\mathrm{SI(a,\,b)} = \sqrt{\frac{[\Sigma_{i=1}^{N}\,(\mathrm{a}_i - \mathrm{b}_i)/\min(\mathrm{a}_i,\,\mathrm{b}_i)]^2}{N}} \times 100$$

where a_i and b_i represent the intensities of the N peaks appearing in the mass spectra of species A and B. Typically, when taking into account the experimental uncertainties, spectra a and b may be considered "identical" for SI(a,b) values less than ~15. Note that this limiting value corresponds to an uncertainty of ±15% on the peak intensities.

Standard ab initio calculations have been carried out using the GAUSSIAN 94 series of programs [14]. The geometries of the different species investigated were first optimized at the HF/6-31G* level; the zero point energy (ZPE) has been calculated at this level after scaling by a factor 0.8929 [15]. The geometries were then refined at the MP2(FrozenCore)/6-31G* level to take electron correlation effects explicitly into account. Restricted (RHF, RMP2) and unrestricted (UHF, UMP2) procedures were used for closed- and open-shell systems, respectively.

It has been established that accurate heats of formation of open-shell systems can be obtained from calculations at the G2 level of theory [16] or its variants, G2(MP2) [17] and G2(MP2,SVP) [18], for species with low spin contamination [19]. For the open-shell species investigated here, the unprojected $\langle S2\rangle$ values were within 0.75–0.78, indicating negligible spin contamination. Owing to the size of the system considered, we decided to choose the G2(MP2,SVP) technique that has been proven to give satisfactory results in this type of system [6]. In the G2(MP2,SVP) theory, the energies are calculated at the QCISD(T) level using the split-valence plus polarization (SVP) 6-31G(d) basis set. Corrections for basis set deficiencies are evaluated at the MP2/6-311+G(3df,2p) level. A higher-level corrections (HLC), that depend on the number of paired and unpaired electrons, is finally introduced. The total energy E[G2(MP2,SVP)] is given by:

$$\begin{aligned}\mathrm{E[G2(MP2,SVP)]} &= \mathrm{E[QCISD(T)/6\text{-}31G(}d\mathrm{)]}\\ &\quad + \mathrm{E[MP2/6\text{-}311{+}G(3}df,2p\mathrm{)]}\\ &\quad - \mathrm{E[MP2/6\text{-}31G(}d\mathrm{)]} + \mathrm{HLC} + \mathrm{ZPE}\end{aligned}$$

The HLC correction is calculated from:

$$\mathrm{HLC} = -A\, n_\beta - B\, n_\alpha$$

Table 1
CA (O_2) spectra of the molecular ions of cyclopropane, propene, and of the [**1**-H_2O]$^+$ ions produced in the ion source (**1**S) (accelerating voltage: 8 kV)

m/z	41	40	39	38	37	36	28	27	26	25	24	16	15	14	13	12
Cyclopropane	72	27	100	27	17	3	10	100	50	14	5	1	100	56	20	5
Propene	68	31	100	29	19	3	14	100	55	18	7	3	100	63	28	11
1S	68	24	100	29	18	3	11	100	52	16	6	2	100	59	16	3

with n_β and n_α being the number of β and α valence electrons, respectively ($n_\beta < n_\alpha$), and the parameters A and B equal to 5.13 10^{-3} and 0.19 10^{-3} Hartree, respectively [18].

RRKM calculations were done using the Stein–Rabinovitch algorithm [20] to estimate the sums,

$$\sum P_{\mathbf{i/j}}{}^{\ddagger}(E{-}E_0)$$

and the densities $N_{\mathbf{j}}(E)$, of vibrational states associated with the single rate coefficient $k_{\mathbf{i}\rightarrow\mathbf{j}}$:

$$k_{\mathbf{i}\rightarrow\mathbf{j}} = \sum P_{\mathbf{i/j}}{}^{\ddagger}(E{-}E_0)/h \cdot N_{\mathbf{i}}(E)$$

The normal mode frequencies given by molecular orbital calculations were used in these calculations (HF/6-31G* scaled by a factor of 0.8953 [15], torsional modes were treated as low-frequency vibrations). For orbiting transition state calculations [21] the rotational constants were obtained from the optimized MP2/6-31G* geometries.

3. Results and discussion

3.1. Tandem mass spectrometry experiments

The behavior of ionized propene and ionized cyclopropane upon collisional conditions has been investigated using collisional activation (CA), charge stripping (CS) and neutralization–reionization (NR) mass spectra. In order to complement the information afforded by these spectra, ion–molecule reactions at near thermal energies of the *m/z* 42 ions with dimethyl disulfide, ammonia, or nitric oxide have also been investigated. The choice of these particular reagents was based on previous data indicating that they allow the identification of ions presenting a distonic character like the ring-opened molecular ion of cyclopropane. All the experiments have been performed on the six sector tandem mass spectrometer at the University of Mons (see Sec. 2).

3.2. Collisional activation spectra

In agreement with previous data [22,23], the high energy CA spectra of ionized cyclopropane and propene are found to be too close to allow a clear identification of these structures. This is attested to by a similarity index, SI(Cy,Pr) = 54, only marginally above the limit under which two spectra may be considered identical owing to the experimental uncertainties (SI ≈ 15). Obviously, the same observation stands for the ionized dehydration product of ionized propanol (Table 1).

3.3. Charge stripping spectra

As already observed [22,23] the most intense peak of the CS spectra (Table 2) corresponds to $C_3H_4^{2+}$ ions (*m/z* 20) and a slightly more intense signal at *m/z* 20.5

Table 2
CS (O_2) mass spectra of $[C_3H_6]^{\cdot+}$ ions from cyclopropane, propene, and propanol, either in the ion source (**1**S) or in the field-free region (**1**m*)

m/z	21	20.5	20	19.5	19
Cyclopropane	2	10	38	24	26
Propene	5	15	31	24	25
1S	1	8	42	22	27
1S, 5600 eV[a]	3	15	41	21	20
1m*	4	19	33	21	23

[a] **1**S, 5600 eV means that the $[C_3H_6]^{\cdot+}$ ions produced in the ion source by dissociative ionization of propanol are subjected to an accelerating voltage of 5600 V; their kinetic energy is thus equal to that of $[C_3H_6]^{\cdot+}$ ions produced in the field-free region from ionized propanol **1** of 8000 eV kinetic energy.

Table 3
Part of the NR (XeO_2) mass spectra of $[C_3H_6]^{\cdot+}$ ions from cyclopropane, propene, and propanol, either in the ion source (**1**S) or in the field-free region (**1**m*)

m/z	42	41	40	39	38	37	36
Cyclopropane	7	24	11	32	13	10	3
Propene	20	17	9	30	12	9	2
1S	19	26	10	27	9	7	2
1S, 5600 eV[a]	22	33	11	23	7	4	1
1m*	19	32	11	24	7	5	1

[a] See footnote to Table 2.

is observed in the case of propene. The SI(Cy,Pr) is equal to 105.

If one considers the relative abundances of the various signals, a better correlation is found between the spectra of ionized cyclopropane ions and the product of dehydration of propanol in the ion source. However, the comparison is not perfect: the SI(Cy, **1**S) is equal to 41, i.e. a value larger than the limiting value of ≈15. When looking at the $[\mathbf{1}\text{-}H_2O]^{\cdot+}$ ions produced in the field-free region, a significant increase of the *m/z* 20.5 signal is observed. Part of this increase is apparently related to the reduced kinetic energy of the ions as attested to by the CS spectrum of source produced $[\mathbf{1}\text{-}H_2O]^{\cdot+}$ ions of 5600 eV kinetic energy. The similarity index between the two latter spectra, SI(**1**m*, **1**S,5600), is equal to 18, indicating that the $[\mathbf{1}\text{-}H_2O]^{\cdot+}$ ions produced either in the ion source or in the field-free region behave comparably. It appears difficult to assign unambiguously a structure to the investigated $[C_3H_6]^{\cdot+}$ ions; the less hazardous conclusion is that no pure ionized propene is produced by water loss from propanol, and that formation of a mixture of cyclopropane and propene is more probable. Moreover, the composition of this mixture appears to be similar at high and low internal energy of the precursor ion **1**.

3.4. Neutralization–reionization spectra

The relative intensity of the recovery signal is lower in the NR spectrum of cyclopropane ions than in the spectrum of propene ions (Table 3). The other signals have a similar appearance and for this reason the SI(Cy,Pr) is not very large [SI(Cy,Pr) = 69]. At first sight, the recovery signal for the ions derived from propanol in the ion source matches that of ionized propene more accurately. This is confirmed by a SI(**1**S,Pr) value of 28. In fact, it is observed that the *m/z* 42:*m/z* 41 ratio is of diagnostic significance with a value is 0.3 for cyclopropane and 1.2 for propene. For the $[C_3H_6]^{\cdot+}$ ions originating from propanol, the *m/z* 42:*m/z* 41 ratio is equal to 0.7. This value, intermediate between that of cyclopropane and propene, may be accounted for by a mixture of both structures. It should be noted that the spectra of the 5600 eV energy ions (source or field-free region) are very similar [SI(**1**S,5600,**1**m*) = 15], pointing again to the formation of the same mixture of structures in both regions.

3.5. Ion–molecule reactions

3.5.1. Ion–molecule reactions with dimethyl disulfide (DMDS)

All the $[C_3H_6]^{\cdot+}$ radical cations react with DMDS by charge exchange producing *m/z* 94 ions. This is in keeping with the relative ionization energies: 9.86 eV for cyclopropane [24], 9.73 eV for propene [24], and 8.18 eV for DMDS [25]. Transfer of a methylthio radical to ionized cyclopropane is not observed and therefore these reactions do not allow the identification of the isomeric $[C_3H_6]^{\cdot+}$ ions.

3.5.2. Ion–molecule reactions with ammonia

Ionized methylene transfer to ammonia starting from ionized cyclopropane has already been reported [26] and is indeed clearly reproduced on our hybrid tandem mass spectrometer. Proton transfer is also

Table 4
Ion–molecule reactions of $[C_3H_6]^{\cdot+}$ ions from cyclopropane, propene, and propanol (either in the ion source, **1**S, or in the field-free region, **1**m*), with ammonia (abundances ratios measured for the methylene transfer and the proton transfer reactions)

	m/z 31:*m/z* 18
Cyclopropane	3.6
Propene	0.06
1S	0.7
1m*	0.3

observed forming *m/z* 18 ions. In the case of propene ions, the proton transfer is the dominant process, however, a small peak is still observed at *m/z* 31, but the ratio *m/z* 31:*m/z* 18 is significantly different from that measured for ionized cyclopropane (Table 4).

It appears from the examination of Table 4 that the behavior of the $[\mathbf{1}\text{-}H_2O]^{\cdot+}$ ions formed in the ion source or in the field-free region is comparable. The *m/z* 31:*m/z* 18 ratio is clearly intermediate between that of cyclopropane and propene. It may thus be concluded that a mixture of both structures is produced in both cases.

3.5.3. Ion–molecule reaction with nitric oxide

Nitric oxide has been used in some instances for the characterization of distonic or distonic-like species; transfer of ionized methylene from ionized cyclopropane to nitric oxide has been observed [27]. In this work, however, charge exchange (*m/z* 30) is by far the most favourable process (Table 5).

Ionized propene does not transfer a methylene group at all to nitric oxide. The behavior of the source produced $[\mathbf{1}\text{-}H_2O]^{\cdot+}$ ions is intermediate between that of cyclopropane and that of propene. The ions formed in the field-free region also react via both reaction channels but the formation of *m/z* 44 ions is notably enhanced with respect to cyclopropane. Only a mixture of cyclopropane and propene structures could explain all these observations.

Table 5
Ion–molecule reactions of $[C_3H_6]^{\cdot+}$ ions from cyclopropane, propene, and propanol (either in the ion source, **1**S, or in the field-free region, **1**m*), with NO (abundance ratios measured for charge exchange and methylene transfer reactions)

	m/z 30:*m/z* 44
Cyclopropane	9
Propene	no peak at *m/z* 44
1S	28
1m*	1.5

3.6. Conclusion

In summary, collisional activation at high kinetic energy appears to be of limited use for the characterization of cyclopropane and propene molecular ions. Less ambiguous conclusions are derived from the NRMS mass spectra. More convincing indications are provided by ion–molecule reactions using ammonia and nitric oxide which demonstrate efficient and specific behaviour for ionized cyclopropane or ionized propene.

The main conclusion of this experimental study is that the $[C_3H_6]^{\cdot+}$ ions produced by water loss from propanol, **1**, react as a mixture of ionized cyclopropane and propene. Moreover, the composition of the mixture seems to be roughly independent of the lifetime of the decomposing ions.

4. Molecular orbital calculations

A detailed investigation of the reaction paths presented in Scheme 1 has been done by means of ab initio molecular orbital calculations. Four minima were located on the MP2/6-31G* potential energy surface: conventional structure **1**, distonic ion **2**, ion-neutral complex between ionized cyclopropane and water, **3**, and a covalently bonded association between ionized propene and water: the distonic ion **4**. The optimized MP2(fc)/6-31G* geometries of these different stationary points and the transition structures connecting them are presented in Fig. 1. The corresponding total and relative energies estimated at various levels of theory are summarized in Table 6.

A general view of the reactions considered is given in Scheme 2.

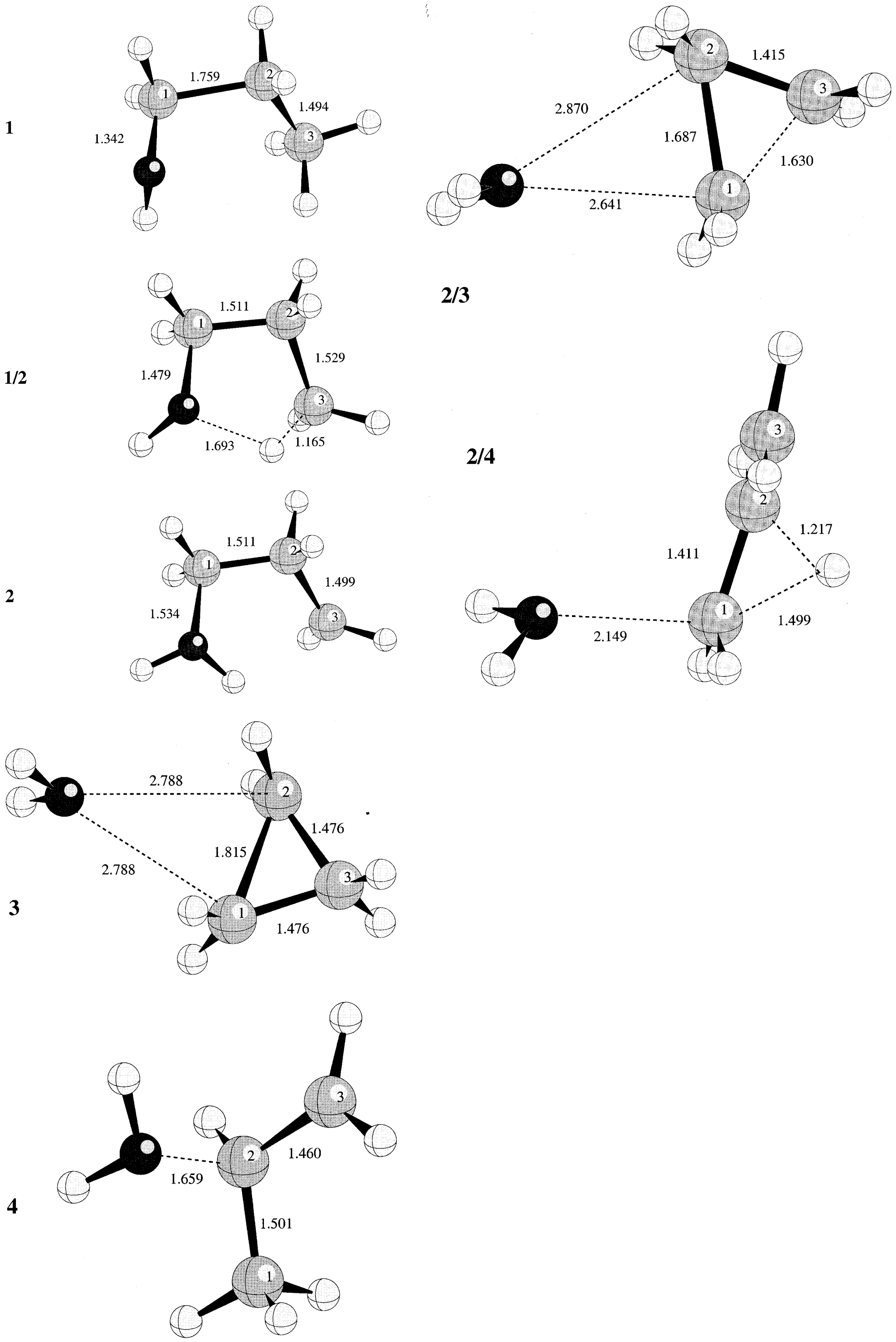

Fig. 1. Optimized MP2/6-31G* geometries of the relevant stationary points of the $[C_3H_8O]^{\cdot+}$ potential energy surface (bond lengths in Å, bond angles in degrees).

Table 6
Total energy (Hartree) for structure **1** and relative energies (kJ/mol) of species **1–6** calculated at various levels of theory

	1	**2**	**1/2**	**3**	**4**	**2/3**	**2/4**	**5**	**6**
HF/6-31G*	−192.77451 0	−53	86	−13	−89	11	27	38	−21
ZPE[a] ($\Delta H°$ 298 K)[b]	265 (284)	268 (282)	260 (274)	257 (278)	257 (278)	259 (273)	248 (268)	251 (272)	249 (270)
MP2/6-31G*	−193.33031 0	−16	110	32	−35	38	80	94	53
QCISD(T)/6-31G*	−193.39365 0	−14	76	30	−35	40	75	91	48
MP2/6-311+G(3*df*,2*p*)	−193.58556 0	−23	115	17	−40	21	58	68	29
G2(MP2,SVP) 0 K	−193.601202 0	−18	76	7	−48	17	36	51	8
G2(MP2,SVP) 298 K	0	−25	71	9	−46	12	37	52	9

[a] From HF/6-31G* vibrational frequencies scaled by a factor of 0.893.

[b] Contribution to enthalpy (ZPE + ΔE_{vib} + $4 \cdot RT$) at 298 K, the factor 0.9135 has been used to estimate the ΔE_{vib} term.

The first step of the reaction, **1** → **2**, has been studied previously [6] and thus only a brief comment is given here. The MP2/6-31G* structure of ionized propanol **1** exhibits a long C(1)–C(2) bond (1.759 Å, Fig. 1) and a short C(1)–O bond (1.342 Å). This situation has been also observed at the MP2/6-31G** level [8]. The most stable form of the distonic ion **2** presents a "gauche" conformation. In this situation a stabilizing interaction is allowed between one of the O-bonded hydrogens (which bears a large positive charge) and the *p* orbital of the carbon atom C(3) (Fig. 1) where the lone electron is located (which constitutes a polarizable centre). The 298 K heats of formation of **1** and **2** have been calculated at the G2(MP2,SVP) level, using atomization and dissociation reactions [6]. The values obtained, $\Delta_f H°(\mathbf{1}) = 713 \pm 4$ kJ mol^{-1} and $\Delta_f H°(\mathbf{2}) = 688 \pm 4$ kJ mol^{-1}, reveal that, as suggested by Baer et al. [8], the

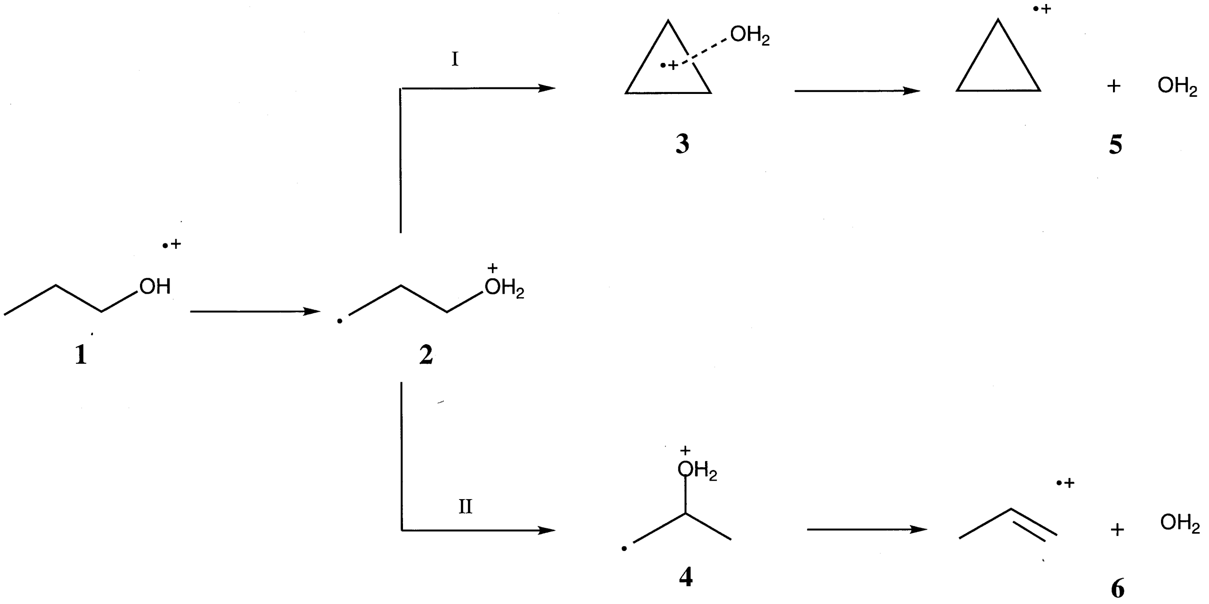

Scheme 2.

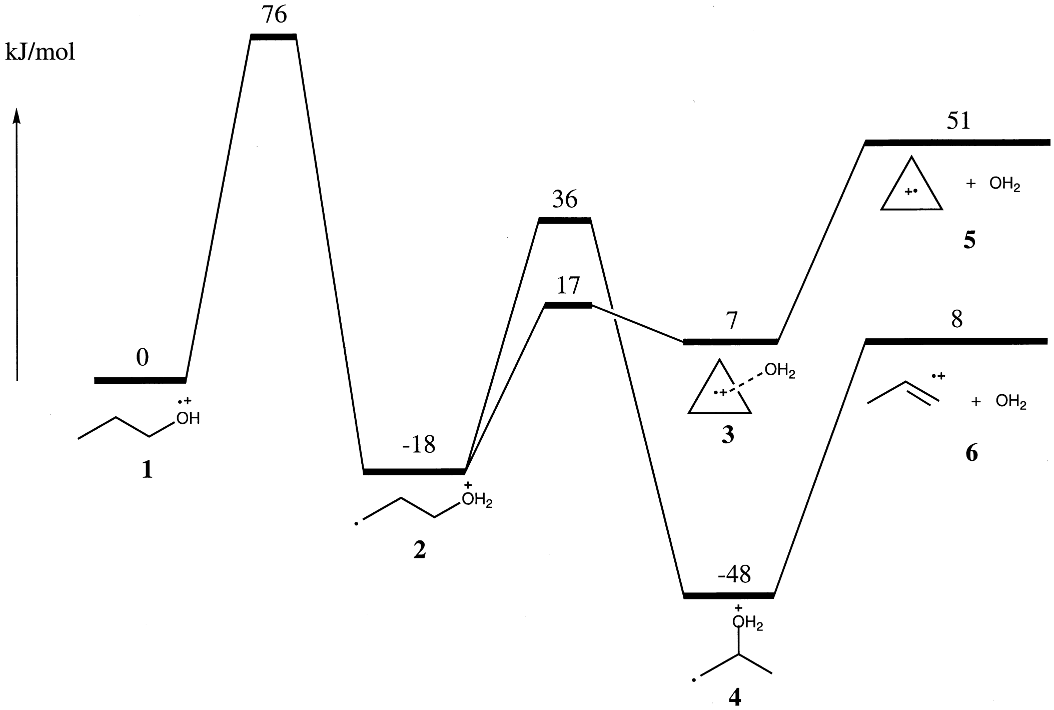

Fig. 2. Potential energy diagram for isomerization and water loss processes from ionized propanol, **1** [G2(MP2,SVP) results, kJ mol^{-1}].

tabulated values (731 and 714 kJ mol^{-1}, respectively) [24] are overestimated.

The calculated transition structure **1/2** adopts a half-chair conformation with O . . . H and C . . . H distances (1.693 Å and 1.165 Å, respectively) close to those encountered in the reactant nearest in energy, i.e. ionized propanol **1**. This 1,4-hydrogen migration is predicted to have an activation barrier of 71 kJ mol^{-1}. By using the G2(MP2,SVP) heat of formation value recalled above, $\Delta_f H°(\mathbf{1}) = 713$ kJ mol^{-1}, we obtain $\Delta_f H°(\mathbf{1/2}) = 784$ kJ mol^{-1} in correct agreement with the experimental threshold measured for the dehydration of ionized propanol (776 kJ mol^{-1}) [5]. As it will be seen below, this 1,4-hydrogen migration **1** → **2** is confirmed to be the energy determining step of the dehydration of ionized propanol (Fig. 2).

Before entering into the description of the reaction channel I (Scheme 2) it is instructive to recall a structural peculiarity concerning ionized cyclopropane. The most stable structure of this species corresponds to a $^2A_1$ electronic state in which one CC bond is lengthened. Accordingly, the MP2/6-31G* optimized geometry of ionized cyclopropane contains two CC bonds of 1.476 Å and one of 1.830 Å. In channel I, water loss from the distonic ion **2** is achieved by a CO bond elongation coupled with a cyclisation process. We thus investigated a reaction path in which, starting from **2**, the C(1)–C(3) distance is progressively shortened. It is observed that, simultaneously, the C(1)–O and the C(1)–C(2) bonds are lengthened whereas the OC(1)C(2) bond angle decreases. At a C(1)–C(3) distance of 1.63 Å the potential energy passes through a maximum and, at smaller distances, it slightly decreases until finally falling into a local minimum corresponding to the ion-neutral complex **3**. In this symmetrical structure, the water molecule interacts with one CC bond of the cyclopropane cation in the CCC plane. Note that the CC bond concerned [C(1)–C(3), Fig. 1] is the longest of the cyclopropane ring, its value (1.815 Å) being slightly lower in the complex than in the isolated ion. The G2(MP2,SVP) energy of **3** with respect to the separated products (the "complexation energy") is equal to 44 kJ mol^{-1}. A comparable value was obtained from experiments [5] and estimated from previous theoretical calculations [8]. The transition structure connecting **2** and **3** (**2/3**) is situated only 10 kJ mol^{-1} above **3** and consequently closely resembles this latter structure (Fig. 1). The formation of ionized cyclopropane plus a water molecule, the final state **5**, is a simple separation of the components of complex **3**. This process is not expected to be associated with a reverse energy barrier and thus the energy requirement for dissociation of **2** into **5** is only the endothermicity of the reaction. The continuous increase of the potential energy during the step **3** → **5** is confirmed by the calculation in which the water-cyclopropane distance is progressively increased. However, we were not able to cleanly characterize a transition structure for this dissociation step.

Reaction II (Scheme 2) involves a 1,2-hydrogen shift concomitant with the water loss from structure **2**. This reaction path has been explored by progressively moving one H atom from C(2) to C(1) (Fig. 1). As a consequence, the C(1)–O bond simultaneously increases. During this process, the potential energy rises rapidly until arriving at a maximum corresponding to the transition structure **2/4**. In this latter, the C–H bond to be broken [C(2)–H] is shorter than that to be formed [C(1)–H] and the water molecule, rather than escaping from the nascent propene molecular ion, begins to move toward C(2). After passing the point **2/4**, the potential energy falls quickly because two bonds are being created in structure **4**: C(1)–H and C(2)–O. Structure **4** is the point of lowest energy in the part of the potential energy surface explored for the present study. This structure is a distonic ion, as attested to by the strong localization of the radical centre on C(3). The C(2)–O and C(2)–C(3) bond lengths (1.659 Å and 1.460 Å, respectively) are very close to the values found for the homolog distonic ion $[CH_2CH_2OH_2]^{\cdot+}$ at the same level of theory (1.613 Å and 1.459 Å) [28]. The last step of the reaction II is the C(2)–O bond elongation which, as for the dissociation of complex **3**, is a process continuously endothermic. No reverse activation barrier is evidenced by the calculations, and as usual in these circumstances, no transition structure could be found by the procedures implemented in the Gaussian routines.

In summary, the G2(MP2,SVP) calculations presented above demonstrate that the dehydration of ionized propanol may occur by two energetically accessible pathways. For both reactions, the energy determining step is the preliminary 1,4-hydrogen migration **1** → **2**. All the distonic ions **2** thus produced have enough energy to undergo water elimination to form either ionized cyclopropane or ionized propene. In the first case, the energy barrier starting from **2** is simply the corresponding endothermicity (i.e. 69 kJ mol^{-1}). In the second case, the energetic barrier corresponding to the isomerisation **2** → **4** (i.e. 54 kJ mol^{-1}) is higher than the exothermicity. Consequently, from a strictly energetic point of view, the formation of ionized propene is expected to be more favourable than ionized cyclopropane. Obviously, the kinetic aspects of the two possible dehydration channels need to be examined further in order to understand the experimental observations. This is the subject of the next section.

5. Statistical rate constant calculations

The kinetic aspects of the water loss from **1** may be investigated further by RRKM calculations of unimolecular rate coefficients on the ab initio potential energy surface of Fig. 2. Because both reactions I and II are initiated by the common step **1** → **2**, it is of interest first to examine the two dissociation channels of the distonic ions **2**.

The rate coefficients, $k_{\mathbf{2\to5}}$ and $k_{\mathbf{2\to6}}$ for the two step processes $\mathbf{2} \rightleftarrows \mathbf{3} \to \mathbf{5}$ and $\mathbf{2} \rightleftarrows \mathbf{4} \to \mathbf{6}$ may be approximated by the steady-state expressions:

$$k_{\mathbf{2\to5}} = (k_{\mathbf{2\to3}} \cdot k_{\mathbf{3\to5}})/(k_{\mathbf{2\to3}} + k_{\mathbf{3\to2}} + k_{\mathbf{3\to5}})$$

$$k_{\mathbf{2\to6}} = (k_{\mathbf{2\to4}} \cdot k_{\mathbf{4\to6}})/(k_{\mathbf{2\to4}} + k_{\mathbf{4\to2}} + k_{\mathbf{4\to6}})$$

where the $k_{\mathbf{i\to j}}$ terms represent the elementary rate constants for the $\mathbf{i} \to \mathbf{j}$ reactions.

Complex **3** is separated from the distonic ion **2** by an energy barrier smaller than the critical energy associated with **3** → **5**. This leads to the inequality $k_{\mathbf{3}\to\mathbf{2}} \gg k_{\mathbf{3}\to\mathbf{5}}$. On the other hand, $k_{\mathbf{2}\to\mathbf{3}}$ must be greater than $k_{\mathbf{3}\to\mathbf{5}}$ because (1) the critical energy of the former process is smaller and (2) ion **3** is less stable than **2** (by 25 kJ mol^{-1}). Consequently the internal energy content of an ion **3** is necessarily less than that of its precursor ion **2**.

The rate coefficient $k_{\mathbf{2}\to\mathbf{5}}$ thus reduces to:

$$k_{\mathbf{2}\to\mathbf{5}} = \sum P_{\mathbf{3/5}}{}^{\ddagger}(E{-}E_{0\mathrm{I}})/h \cdot N_{\mathbf{2}}(E)$$

where $E_{0\mathrm{I}}$ is the energy difference between **2** and **5**. This expression is that for a rate constant involving reactant **2** and transition structure **3/5**. Unfortunately it has been shown that the flatness of the potential energy surface near the dissociation limit prevents us from locating a transition structure **3/5**. In such a situation it is preferable to use a theory that is able to model barrierless dissociations and needs only characteristics of the products in the estimation of the sum and density of vibrational–rotational states. Thus, in order to evaluate $k_{\mathbf{2}\to\mathbf{5}}$, we have used the statistical phase space theory developed by Chesnavich et al. [21].

The highest stability of **4** with respect to **2** (30 kJ mol^{-1}) results in the inequality $k_{\mathbf{2}\to\mathbf{4}} \gg k_{\mathbf{4}\to\mathbf{2}}$. Further, for the same reason, any ion **2** of internal energy E leads to an ion **4** of internal energy $E' = E + 30$ kJ/mol. Thus the two rate coefficients $k_{\mathbf{2}\to\mathbf{4}}$ and $k_{\mathbf{4}\to\mathbf{6}}$ that possess similar critical energies are in the order $k_{\mathbf{2}\to\mathbf{4}} \ll k_{\mathbf{4}\to\mathbf{6}}$. This is particularly true at low internal energy. Consequently, to a good approximation, we can consider that:

$$k_{\mathbf{2}\to\mathbf{6}} = k_{\mathbf{2}\to\mathbf{4}} = \sum P_{\mathbf{2/4}}{}^{\ddagger}(E{-}E_{0\mathrm{II}})/h \cdot N_{\mathbf{2}}(E)$$

with $E_{0\mathrm{II}}$ being the critical energy for the reaction **2** → **4**.

The resulting rate coefficients $k_{\mathbf{2}\to\mathbf{5}}$ and $k_{\mathbf{2}\to\mathbf{6}}$ calculated under these conditions, and using the G2(MP2,SVP) critical energy values $E_{0\mathrm{I}} = 69$ kJ mol^{-1} (0.71 eV) and $E_{0\mathrm{II}} = 54$ kJ mol^{-1} (0.56 eV), are presented in Fig. 3.

As demonstrated by these plots, the calculation indicates that, very rapidly above 0.8 eV, $k_{\mathbf{2}\to\mathbf{5}}$ and $k_{\mathbf{2}\to\mathbf{6}}$ are of the same order of magnitude. In fact, the use of the orbiting transition state theory allows the reaction rate coefficient $k_{\mathbf{2}\to\mathbf{5}}$ to be greater than $k_{\mathbf{2}\to\mathbf{6}}$ in an internal energy range of ~1.5 eV. It is clear that starting from **2** or from **1** the formation of a mixture of ionized propene and cyclopropane is expected. This is particularly true for dissociating ions **1**, which necessarily have internal energy larger than the barrier for 1,4-H migration **1** → **2** (vertical bar at $E = 0.98$ eV in Fig. 3).

The overall rate constant for the net dehydration reaction of **1** to give **5** and **6**, may be approximated by:

$$k_{\mathrm{dehydr}} = (k_{\mathbf{1}\to\mathbf{2}})(k_{\mathbf{2}\to\mathbf{5}} + k_{\mathbf{2}\to\mathbf{6}})/(k_{\mathbf{1}\to\mathbf{2}} + k_{\mathbf{2}\to\mathbf{1}} + k_{\mathbf{2}\to\mathbf{5}} + k_{\mathbf{2}\to\mathbf{6}})$$

Simple calculation shows that the term $k_{\mathbf{2}\to\mathbf{5}} + k_{\mathbf{2}\to\mathbf{6}}$ is greater than $k_{\mathbf{1}\to\mathbf{2}}$ or $k_{\mathbf{2}\to\mathbf{1}}$ by no less than five orders of magnitude. One may consequently write $k_{\mathrm{dehydr}} = k_{\mathbf{1}\to\mathbf{2}}$; the corresponding curve is also presented in Fig. 3. It can be seen that k_{dehydr} starts from a value close to $10^6\ \mathrm{s}^{-1}$ and rises very slowly with internal energy, attaining only $10^{11}\ \mathrm{s}^{-1}$ for $E = 5.0$ eV. A comparison of the k_{dehydr} versus E curve with the experimental data reported by Baer et al. [5,29] is instructive. The authors determined the dissociation rate of energy selected propanol ions by photoelectron photoion coincidence measurement. They observed that this rate ranges between $2.10^5\ \mathrm{s}^{-1}$ and $2.10^6\ \mathrm{s}^{-1}$ near the dissociation threshold, clearly in agreement with our calculated minimum rate constant value of $10^6\ \mathrm{s}^{-1}$. This agreement indirectly confirms the validity of the coupled RRKM/MO approach used in the present study.

6. Conclusion

Several pieces of evidence are presented supporting the view that the dehydration of ionized propanol not only produces ionized cyclopropane but also ionized propene. Charge stripping and neutralisation–reionization mass spectra and, principally, ion–molecule reactions with ammonia and NO, are best

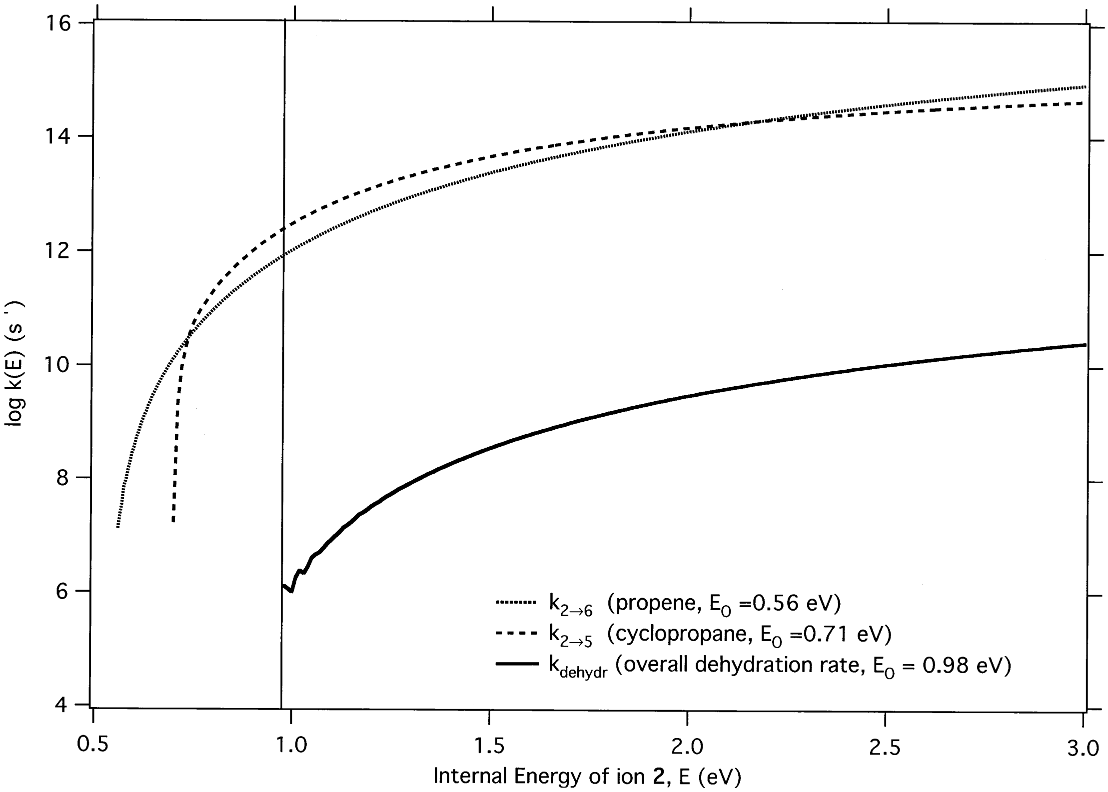

Fig. 3. Statistical rate constants for dehydration reactions from distonic ion $[CH_2CH_2CH_2OH_2]^{\cdot+}$, **2**, and overall water loss from ionized propanol, **1**.

understood if a mixture of the two $[C_3H_6]^{\cdot+}$ ion structures is produced. Molecular orbital calculations at a reasonably high level of theory, G2(MP2,SVP), show that the formation of ionized propene is energetically favoured. Detailed statistical rate constant calculations demonstrate that the two dehydration routes are essentially competitive in all internal energy regimes, even if the loose nature of the dissociating structure leading to ionized cyclopropane is fully taken into account by an orbiting transition state model.

References

[1] J.L. Holmes, A.A. Mommers, J.E. Szulejko, J.K. Terlouw, J. Chem. Soc. Chem. Commun. (1984) 165.
[2] R.D. Bowen, A.W. Colburn, P.J. Derrick, J. Am. Chem. Soc. 113 (1991) 1132.
[3] V. Wysocki, H.I. Kenttämaa, J. Am. Chem. Soc. 112 (1990) 5110.
[4] C. Wesdemiotis, P.O. Danis, R. Feng, J. Tso, F.W. McLafferty, J. Am. Chem. Soc. 107 (1985) 8059.
[5] J.D. Shao, T. Baer, J.C. Morrow, M.L. Fraser-Monteiro, J. Chem. Phys. 87 (1987) 5242.
[6] G. Bouchoux, N. Choret, unpublished.
[7] T. Takeuchi, S. Ueno, M. Yamamoto, T. Matsushita, K. Nishimoto, Int. J. Mass Spectrom. Ion Processes 64 (1985) 33.
[8] J.A. Booze, T. Baer, J. Phys. Chem. 96 (1992) 5710.
[9] J.A. Booze, T. Baer, J. Phys. Chem. 96 (1992) 5715.
[10] A. Skancke, J. Phys. Chem. 99 (1995) 13 886.
[11] R.H. Bateman, J. Brown, M. Lefevre, R. Flammang, Y. Van Haverbeke, Int. J. Mass Spectrom. Ion Processes 115 (1992) 205.
[12] R. Flammang, Y. Van Haverbeke, C. Braybrook, J. Brown, Rapid Commun. Mass Spectrom. 9 (1995) 795.
[13] J.O. Lay, M.L. Gross, J.J. Zwinselman, N.M.M. Nibbering, Org. Mass Spectrom. 18 (1983) 16.
[14] M.J. Frisch, G.W. Trucks, H.B. Schlegel, P.M.W. Gill, B.G. Johnson, M.A. Robb, J.R. Cheesemann, T.A. Keith, G.A.

Petersson, J.A. Montgomery, K. Raghavachari, M.A. Al-Laham, V.G. Zakrewski, J.V. Ortiz, J.B. Foresman, J. Cioslowski, B.B. Stefanov, A. Nanayakkara, M. Challacombe, C.Y. Peng, P.Y. Ayala, W. Chen, M.W. Wong, J.L. Andres, E.S. Replogle, R. Gomperts, R.L. Martin, D.J. Fox, J.S. Binkley, D.J. Defrees, J. Baker, J.P. Stewart, M. Head-Gordon, C. Gonzales, J.A. Pople, GAUSSIAN 94, Gaussian, Inc., Pittsburgh, PA, 1995.

[15] (a) A.P. Scott, L. Radom, J. Phys. Chem. 100 (1996) 16 502; (b) J.A. Pople, A.P. Scott, M.W. Wong, L. Radom, Israel. J. Chem. 33 (1993) 345.

[16] L.A. Curtiss, K. Raghavachari, G.W. Trucks, J.A. Pople, J. Chem. Phys. 94 (1991) 7221.

[17] L.A. Curtiss, K. Raghavachari, J.A. Pople, J. Chem. Phys. 98 (1993) 1293.

[18] (a) B.J. Smith, L. Radom, J. Phys. Chem. 99 (1995) 6468; (b) L.A. Curtiss, P.C. Redfern, B.J. Smith, L. Radom, J. Chem. Phys. 104 (1996) 5148.

[19] P.M. Mayer, C.J. Parkinson, D.M. Smith, L. Radom, J. Chem. Phys. 108 (1998) 604.

[20] (a) T. Beyer, D.R. Swinehard, ACM Commun. 16 (1973) 379; (b) S.E. Stein, B.S. Rabinovitch, J. Chem. Phys. 58 (1973) 2438.

[21] W.J. Chesnavich, L. Bass, M.E. Grice, K. Song, D.A. Webb, Quantum Chemistry Program Exchange (QCPE) 557 program.

[22] R.D. Bowen, M.P. Barbalas, F.P. Pagano, P.J. Todd, F.W. McLafferty, Org. Mass Spectrom. 15 (1980) 51.

[23] J.L. Holmes, J.K. Terlouw, P.C. Burgers, R.T.B. Rye, Org. Mass Spectrom. 15 (1980) 149.

[24] S.G. Lias, J.E. Bartmess, J.F. Liebman, J.L. Holmes, R.D. Levin, W.G. Mallard, J. Phys. Chem. Ref. Data 17 (1988) Suppl. 1.

[25] C.Y. Ng, in The structure, energetics and dynamics of organic ions, T. Baer, C.Y. Ng, I. Powis (Eds.), Wiley, New York, 1996, p. 62.

[26] (a) M.L. Gross, F.W. McLafferty, J. Am. Chem. Soc. 93 (1971) 1267; (b) L.K.M. Kiminkinen, H.I. Kenttämaa, Chem. Rev. 92 (1992) 1649.

[27] T. Weiske, H. van der Wel, N.M.M. Nibbering, H. Schwarz, Angew. Chem. Int. Ed. Engl. 23 (1984) 733.

[28] J.W. Gauld, L. Radom, Chem. Phys. Lett. 275 (1997) 28.

[29] T. Baer, in The structure, energetics and dynamics of organic ions, T. Baer, C.Y. Ng, I. Powis (Eds.), Wiley, New York, 1996, p. 149.